J. Fluid Mech. (1983), *vol.* 132, *pp.* 283–293
Printed in Great Britain

An algorithmic approach to the linear stability of the Ekman layer

By MOGENS V. MELANDER

Laboratory of Applied Mathematical Physics and Institute for Numerical Analysis, Technical University of Denmark

(Received 20 January 1982 and in revised form 4 February 1983)

The linear stability of the stationary Ekman-layer flow near a plane boundary is considered. Analytical formulas for the eigenfunctions are derived by a spectral analysis. Standard optimization algorithms are used to calculate critical points, maximum growth rates and neutral-stability curves. The new approach provides a better basis for both a linear and a nonlinear stability analysis than the well-known methods have done. The method may also be applied to other boundary-layer problems.

1. Introduction

The stationary Ekman-layer flow that is known to exist for sufficiently small Reynolds numbers changes into a time-periodic motion consisting of travelling parallel vortex rolls when the Reynolds number is larger than a certain critical value (Faller 1963). Two distinct modes of instability are observed. These were originally designated as type 1 and 2. The first type consists of slowly moving vortices, with axis orientated to the left of the geostrophic flow. In contrast, the second type moves rapidly and has axis orientated to the right of the geostrophic flow, and it appears at a lower Reynolds number. Linear stability theory formulated in terms of an eigenvalue problem for a system of ordinary differential equations furnishes the parameter values at which the instabilities occur. The equations were solved by Faller & Kaylor (1966) and by Lilly (1966) by the use of finite differences. Iooss, Nielsen & True (1978) applied a Galerkin method, with cubic splines as trial functions in order to obtain a better approximation of the eigenfunctions, which are needed in a bifurcation analysis.

As part of a broader nonlinear analysis that is in preparation, the analytical form of the solutions of the linearized problem has been investigated. They appear as series of certain complex exponential functions in connection with a recurrence formula for the coefficients. The series turn out to be uniformly and absolutely convergent. They converge fast and are easy to handle numerically. It is cheaper to solve the problem by these series than to solve it by usual numerical methods, but we do not get *a priori* information about the location of the eigenvalues. However, the stability analysis is formulated in a natural way through optimization problems for a transcendental function that is derived from the series. This formulation proved to be a profitable way to obtain accurate results. All previous results of interest for comparison with a nonlinear analysis are checked.

The objectives of this paper are therefore first to derive analytical expressions for the eigenfunctions, secondly to prove their computational value, and finally to show that linear stability problems can successfully be treated as optimization problems.

2. Formulation of the problem

The flow is described by the Navier–Stokes equations for an incompressible, viscous fluid in a rotating coordinate system situated such that the plane wall is described $Z = 0$

$$\left.\begin{aligned} \frac{\mathrm{d}\boldsymbol{V}}{\mathrm{d}T} &= -\boldsymbol{\nabla}\frac{P}{\rho} - 2\Omega\boldsymbol{k}\times\boldsymbol{V} + \nu\nabla^2\boldsymbol{V}, \\ \boldsymbol{\nabla}\cdot\boldsymbol{V} &= 0. \end{aligned}\right\} \tag{1}$$

We use the following notation:

X, Y, Z	Cartesian coordinates,
T	time,
P	pressure,
$\boldsymbol{V}$	velocity vector,
$\boldsymbol{V}_{\mathrm{H}}$	horizontal projection of the velocity vector,
Ω	angular velocity of the rotation of the coordinate frame (assumed constant),
ρ	density (assumed constant),
$\frac{\mathrm{d}}{\mathrm{d}T}$	total derivative,
$\boldsymbol{k}$	unit vector in the Z-direction.

A condition of no slip is applied at the plane boundary. At the upper surface situated infinitely high over the plane boundary, the vertical component of the velocity and the tangential shear stress vanish:

$$\left.\begin{aligned} \boldsymbol{V} &= 0 \quad \text{at} \quad Z = 0, \\ \boldsymbol{k}\cdot\boldsymbol{V} &= (\boldsymbol{k}\cdot\boldsymbol{\nabla})\,\boldsymbol{V}_{\mathrm{H}} = 0 \quad \text{as} \quad Z\to\infty. \end{aligned}\right\} \tag{2}$$

Replacement of the variables by their scaled counterparts brings the equations into dimensionless form:

$$\left.\begin{aligned} &\frac{\partial\boldsymbol{v}}{\partial t} + (\boldsymbol{v}\cdot\boldsymbol{\nabla})\,\boldsymbol{v} = -\boldsymbol{\nabla}p - \frac{2}{R}\boldsymbol{k}\times\boldsymbol{v} + \frac{1}{R}\nabla^2\boldsymbol{v}, \quad \boldsymbol{\nabla}\cdot\boldsymbol{v} = 0, \\ &\boldsymbol{V} = U\boldsymbol{v}, \quad T = \frac{\delta}{U}t, \quad (X, Y, Z) = \delta(x, y, z), \quad P = \rho U^2 p, \quad R = \frac{U}{(\nu\Omega)^{\frac{1}{2}}} \end{aligned}\right\} \tag{3}$$

U denotes the outer mean velocity, R the Reynolds number and $\delta = (\nu/\Omega)^{\frac{1}{2}}$ is the thickness of the boundary layer. A stationary solution $(\boldsymbol{V}_{\mathrm{b}}, p_{\mathrm{b}})$, known as the Ekman spiral, exists for all values of the Reynolds number; but it is known to be asymptotically stable only for sufficiently small Reynolds numbers:

$$\left.\begin{aligned} \boldsymbol{V}_{\mathrm{b}} &= (1 - \exp(-z)\cos z, \exp(-z)\sin z, 0), \\ \boldsymbol{\nabla}p_{\mathrm{b}} &= \left(0, -\frac{2}{R}, 0\right). \end{aligned}\right\} \tag{4}$$

The linear stability equations are obtained by linearization of the Navier–Stokes equations about this flow. The coordinate system is rotated through some angle ϵ counterclockwise around the z-axis, $(x, y, z)\to(\xi, \eta, z)$, and we investigate banded disturbances $\boldsymbol{u}(t, \eta, z)$, independent of ξ. By introduction of a stream function we can write

$$\boldsymbol{u} = [\mu(z), -\phi'(z), \mathrm{i}\alpha\phi(z)]\exp(\mathrm{i}\alpha(\eta - ct)), \tag{5}$$

where α is the wavenumber and c the complex phase speed. The pressure is eliminated by cross-differentiation, and two coupled oridinary differential equations are obtained:

$$\left.\begin{aligned}&(\mathrm{D}^2-\alpha^2)^2\phi-\mathrm{i}\alpha R[(v_\mathrm{b}-c)(\mathrm{D}^2-\alpha^2)-\mathrm{D}^2v_\mathrm{b}]\phi+2\mathrm{D}\mu=0,\\&(\mathrm{D}^2-\alpha^2)\mu-\mathrm{i}\alpha R[(v_\mathrm{b}-c)\mu+\mathrm{D}u_\mathrm{b}\phi]-2\mathrm{D}\phi=0,\\&\mathrm{D}\equiv\frac{\mathrm{d}}{\mathrm{d}z}.\end{aligned}\right\}\tag{6}$$

The boundary conditions are

$$\phi=\mathrm{D}\phi=\mu=0 \quad \text{at} \quad z=0,$$

$$\phi,\ \mathrm{D}^2\phi, D\mu\to 0 \quad \text{as} \quad z\to\infty.$$

u_b and v_b represent the basic flow in the rotated coordinate system:

$$\left.\begin{aligned}u_\mathrm{b}&=\cos\epsilon-\exp(-z)\cos(z+\epsilon),\\v_\mathrm{b}&=-\sin\epsilon+\exp(-z)\sin(z+\epsilon).\end{aligned}\right\}\tag{7}$$

The equations define an eigenvalue problem which determined c in terms of R, α and ϵ.

3. Construction of solutions

The stability equations (6) are equivalent to six first-order ordinary differential equations. Thus there exist exactly six linearly independent solutions $\boldsymbol{v}_1, \ldots, \boldsymbol{v}_6$. The general solution is a linear combination of these. However, we can arrange the linear combination in such a way that exactly three of the linearly independent solutions, say $\boldsymbol{v}_4$, $\boldsymbol{v}_5$, $\boldsymbol{v}_6$, are unbounded at infinity. These can therefore be omitted. Application of the boundary conditions at the wall leads to three linear homogeneous equations. An eigensolution exists if and only if the corresponding matrix is singular. Hence we have a relation between c and the parameters. In order to find six linearly independent solutions we rewrite (6) in the form

$$(\boldsymbol{C}-\mathrm{i}\alpha R\boldsymbol{G})\boldsymbol{v}=0, \quad \boldsymbol{v}\equiv(\phi,\mu),\tag{8}$$

where

$$\boldsymbol{C}=\begin{pmatrix}(\mathrm{D}^2-\alpha^2)^2+\mathrm{i}\lambda(\mathrm{D}^2-\alpha^2) & 2\mathrm{D}\\ -2\mathrm{D} & \mathrm{D}^2-\alpha^2+\mathrm{i}\lambda\end{pmatrix},$$

$$\lambda=(c+\sin\epsilon)\alpha R,$$

$$\boldsymbol{G}=\exp(-z)\begin{pmatrix}\sin(z+\epsilon)(\mathrm{D}^2-\alpha^2)+2\cos(z+\epsilon) & 0\\ \cos(z+\epsilon)+\sin(z+\epsilon) & \sin(z+\epsilon)\end{pmatrix}.$$

Since the operator $\boldsymbol{G}$ vanishes as z tends to infinity, we try to construct v_1, v_2, v_3 by the following scheme:

$$\boldsymbol{v}=\sum_{m=0}^{\infty}\boldsymbol{u}_m, \quad \boldsymbol{C}\boldsymbol{u}_0=0, \quad \boldsymbol{C}\boldsymbol{u}_m=i\alpha R\boldsymbol{G}\boldsymbol{u}_{m-1}.\tag{9}$$

The zeroth-order equation has solutions in form of complex exponential functions. The characteristic equation

$$(k^2-\alpha^2+\mathrm{i}\lambda)^2(k^2-\alpha^2)+4(k^2-\alpha^2)=-4\alpha^2\tag{10}$$

has exactly six distinct roots ($\alpha \neq 0$), three with positive and three, $k_{00}^{(1)}, k_{00}^{(2)}, k_{00}^{(3)}$, with negative real part. Let these basic modes be numbered after increasing imaginary part. For $\boldsymbol{u}_m$ we find

$$\boldsymbol{u}_m = \sum_{j=0}^{n} a_{nj} \exp\left[(k_{00} - n + \mathrm{i}(2j-n))\, z\right]. \tag{11}$$

From this formula we interpret $\boldsymbol{C}$ as a mode-conserving and $\boldsymbol{G}$ as a mode-generating operator. We shall use a spectral notation for the calculation of a_{nj}. Starting from the basic mode k_{00}, successive use of $\boldsymbol{C}$ and $\boldsymbol{G}$ creates a discrete fan of modes in the k-plane. A relation between the amplitudes a_{nj} and $a_{n-1,j}, a_{n-1,j-1}$ is provided by

$$\left.\begin{aligned} \sum_{j=0}^{n} \boldsymbol{C} a_{nj} \exp(k_{nj} z) = \sum_{j=0}^{n-1} \boldsymbol{G} a_{n-1,j} \exp(k_{n-1,j} z), \\ k_{nj} = k_{00} - n + \mathrm{i}(2j-n). \end{aligned}\right\}$$

These equations show that we can determine the a_{nj} recurrently by using the scheme

$$\left.\begin{aligned} \mathscr{C} a_{00} = 0, \quad \|a_{00}\|_\infty = 1, \\ \mathscr{C} a_{nj} = \mathscr{G}_{\mathrm{up}} a_{n-1,j-1} + \mathscr{G}_{\mathrm{down}} a_{n-1,j}, \end{aligned}\right\} \tag{12}$$

where

$$\mathscr{C} = \begin{pmatrix} (k_{nj}^2 - \alpha^2)^2 + \mathrm{i}\lambda(k_{nj}^2 - \alpha^2) & 2k_{nj} \\ -2k_{nj} & \mathrm{i}\lambda + k_{nj}^2 - \alpha^2 \end{pmatrix},$$

$$\mathscr{G}_{\mathrm{up}} = \frac{\mathrm{i}\alpha R}{2} \exp(\mathrm{i}\epsilon) \begin{pmatrix} -(k_{n-1,j-1}^2 - \alpha^2) + 2 & 0 \\ 1 - \mathrm{i} & -\mathrm{i} \end{pmatrix},$$

$$\mathscr{G}_{\mathrm{down}} = \frac{i\alpha R}{2} \exp(-i\epsilon) \begin{pmatrix} k_{n-1,j}^2 - \alpha^2 + 2 & 0 \\ 1 + \mathrm{i} & \mathrm{i} \end{pmatrix}.$$

We have now constructed three linearly independent solutions of the form

$$\boldsymbol{v}_l = \sum_{n=0}^{\infty} \sum_{j=0}^{n} a_{nj}^{(l)} \exp\left[(k_{00}^{(l)} - n + \mathrm{i}(2j-n))\, z\right] \quad (l = 1, 2, 3), \tag{13}$$

and we shall now investigate the convergence of these series. We therefore consider (12) in the limit as n tends to infinity, in order to get an upper bound for the numerically largest component of a_{nj}:

$$\begin{aligned} \|a_{nj}\|_\infty &= \|\mathscr{C}^{-1}\mathscr{G}_{\mathrm{up}} a_{n-1,j-1} + \mathscr{C}^{-1}\mathscr{G}_{\mathrm{down}} a_{n-1,j}\|_\infty \\ &\leqslant 2 \max\{\|\mathscr{C}^{-1}\mathscr{G}_{\mathrm{up}}\|_\infty, \|\mathscr{C}^{-1}\mathscr{G}_{\mathrm{down}}\|_\infty\} \max_j \|a_{n-1,j}\|_\infty \\ &\leqslant \frac{2\alpha R}{n^2} \max_j \|a_{n-1,j}\|_\infty \\ &\leqslant \frac{2\alpha R}{n!\, n!} \|a_{00}\|_\infty. \end{aligned} \tag{14}$$

When we use this upper bound to estimate the remainder of the series, we find for any fixed value of z

$$\begin{aligned} \left\| \boldsymbol{v}_l - \sum_{n=0}^{N} \boldsymbol{u}_n \right\|_\infty &< (N+1) \max_j \|a_{Nj}^{(l)}\|_\infty \exp\left[(k_{00}^{(l)} - N) z\right] (1 + O(N^{-2})) \\ &\sim N \frac{(2\alpha R)^N}{N!\, N!} \exp(-Nz). \end{aligned} \tag{15}$$

From these calculations we conclude that the series (13) are uniformly and absolutely convergent on the interval $[0, \infty]$. In order to prove that the series are exact solutions to (6), we only have to substitute (13) into the equations, because the convergence properties allow rearrangement of the summations, the operators and the terms. The unbounded solutions v_4, v_5, v_6 can be treated in the same way. The relation between c and α, ϵ, R is now expressed in the following way:

$$\det \boldsymbol{M}(c, \alpha, \epsilon, R) = 0, \tag{16}$$

$$\boldsymbol{M} = \sum_{n=0}^{\infty} \boldsymbol{M}_n, \quad \boldsymbol{M}_n = \sum_{j=0}^{n} \boldsymbol{M}_{nj}, \tag{17}$$

$$M_{nj} = \begin{bmatrix} f_{nj}^{(1)} & f_{nj}^{(2)} & g_{nj}^{(3)} \\ g_{nj}^{(1)} & g_{nj}^{(2)} & f_{nj}^{(3)} \\ k_{nj}^{(1)} f_{nj}^{(1)} & k_{nj}^{(2)} f_{nj}^{(2)} & k_{nj}^{(3)} f_{nj}^{(3)} \end{bmatrix},$$

here we have denoted the components of a_{nj} by

$$a_{nj}^{(l)} = (f_{nj}^{(l)}, g_{nj}^{(l)}) \quad (l = 1, 2, 3).$$

4. Evaluation of the series

We intend to use the formulas (12) and (13) as an algorithm for the three components of the eigenfunction and the determinant of $\boldsymbol{M}$. Therefore the numerical reliability of the algorithm must be verified. This reliability is closely related to the rate of convergence of the series (13). For comparison with the theoretical bound (14), the maximum $\|a_{Nj}\|$ was calculated for different values of N. At each N a constant K was determined such that

$$\max_j \|a_{Nj}\|_\infty = \frac{K^N}{N!\,N!}.$$

From table 1 it is seen that the theoretical bound (14) agrees well with the real rate of convergence, if $2\alpha R$ is replaced by a smaller constant.

N	$\max_j \|a_{Nj}\|$	K	$D_N(c, \alpha, \epsilon, R)$
1	3.19	3.19	9.417560459906 37
2	3.88	3.94	6.344576707469 11
4	9.32′–01	4.81	0.350187867379144
6	1.43′–01	6.48	0.010124641107220
8	3.51′–03	6.99	0.000067114603708
10	2.39′–05	7.08	0.000000128327130
12	6.66′–08	7.06	0.000000000083538
14	1.01′–10	7.06	0.000000000000032
16	9.86′–14	7.12	0.000000000000013
18	6.24′–17	7.18	0.000000000000007
20	2.52′–20	7.22	
25	1.24′–29	7.23	
30	8.52′–40	7.23	

TABLE 1. Convergence properties of the series and the determinant. The parameter values used in the calculation are:

$c_r = 0.616301969005562$, $c_i = 0$, $\alpha = 0.316225064429603$, $\epsilon = -23.326108746469 1°$, $R = 54.155039249992 9$, $l = 3$ in the first and second column.

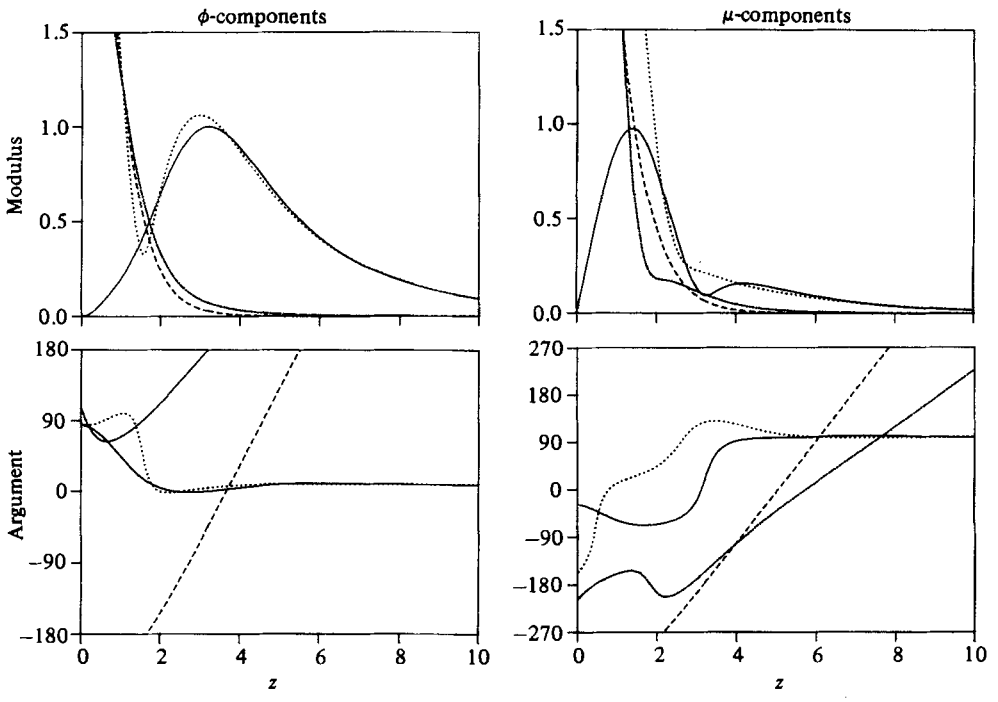

FIGURE 1. Moduli and arguments of the eigenfunction $v = (\phi, \mu)$ (—) and the three components $v_1 = (\phi_1, \mu_1)$ (– – –), $v_2 = (\phi_2, \mu_2)$ (- · - · -) and $v_3 = (\phi_3, \mu_3)$ (...). The three linearly independent solutions are numbered after increasing imaginary part of the corresponding basic mode (see figure 2). The parameter values are the ones for the critical type-2 point. The linear combination giving the eigenfunction is $v = (-2.317 - 0.0843\mathrm{i})\, v_1 + (-0.0094 + 1.664\mathrm{i})\, v_2 + v_3$. This eigenfunction is normalized such that the maximum modulus of ϕ is 1 and the corresponding argument is 0. v_1, v_2 and v_3 increase in norm to about 100 as z tends to zero.

Since (13) allows evaluation of the fundamental matrix, a residue check is possible. It is convenient to measure the residue relative to the norm of the first term in the series (13). Numerical experiments show that the maximum residue occurs near $z = 0$, in agreement with (15), and that at least 12 out of 16 possible decimal figures (the machine accuracy for the IBM-3033 machine) can be obtained correctly. Thus the numerical evaluation of the series is a sound process.

When c is an eigenvalue, we have

$$D_N(c, \alpha, \epsilon, R) \equiv \det \sum_{n=0}^{N} \boldsymbol{M}_n(c, \alpha, \epsilon, R) \to 0 \quad \text{as} \quad N \to \infty.$$

Table 1 shows how well this limit is attained. The results show that an optimum truncation is achieved when the sum $\Sigma_j \|a_{Nj}\|$ becomes comparable to $\|a_{00}\|$ times the machine accuracy. The computational effort involved to evaluate the determinant is about $20(N_1^2 + N_2^2 + N_3^2)$ simple arithmetic operations on complex numbers, where $N_1, \ldots$ denote the indices for truncations of the respective series.

The eigenfunction is a linear combination of v_1, v_2 and v_3. One of these is of inviscid character and dominates the eigenfunction up to a few boundary-layer thicknesses from the wall (see figure 1). The phenomenon is most pronounced for the ϕ-component because the two inviscid ϕ-components almost cancel each other near $z = 1.8$.

Some qualitative information follows from the location of the basic modes $k_{00}^{(1)}$, $k_{00}^{(2)}$, $k_{00}^{(3)}$, which depends only on α and λ. The inviscid basic mode, and therefore all the

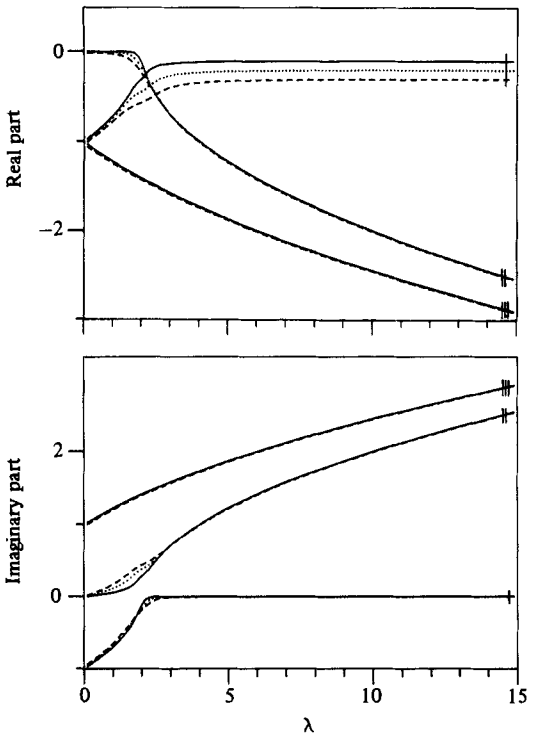

FIGURE 2. Real and imaginary part of the basic modes $k_{00}^{(1)}$, $k_{00}^{(2)}$, and $k_{00}^{(3)}$ are shown as functions of $\lambda = (c+\sin\epsilon)\alpha R$ for $\alpha = 0.3$ (—); 0.6 (.....) and 0.9 (– – – –); on all curves $c_i = 0$. The basic modes are roots in the characteristic polynomial (10). For the critical type-2 point we have $\lambda = 3.77$, $\alpha = 0.316$, and for the critical type-1 point $\lambda = 13.63$ and $\alpha = 0.551$.

modes of the inviscid solution, depends mainly on α, while the viscous modes depend mainly on λ (figure 2). Furthermore it is typical that the inviscid component has constant phase outside the boundary layer. The figure also illustrates the non-coincidence of the three basic modes – a precondition for the validity of (13).

5. Linear stability analysis through optimization

Since we have an algorithm for the evaluation of the determinant, it is obvious that the stability analysis should be formulated through optimization problems. For the solution of such problems there exist efficient algorithms, which require only a few evaluations of the criteria function. The convergence is usually rapid in the neighbourhood of a solution; hence it is economical to achieve a high accuracy. Furthermore, good global convergence properties of the methods allow rough initial guesses.

The growth rate is eliminated at once by putting $c_i = 0$. In order to find a neutral-stability point, two of the parameters, e.g. α and ϵ, are fixed at some reasonable values, and the absolute square of the determinant is minimized in order to find a zero. For this purpose a modified Marquardt algorithm (Powell 1970), which does not require derivatives, is used. There is no guarantee that the point belongs to the lowest eigenstate. However, experience shows that it is usually the case. Typically 30–40 evaluations of the determinant are necessary to find a neutral point starting with values that may be a factor 2 off from the solution. The critical point

Reference	Wave type	R	αc_r	$2\pi/\alpha$	ϵ
Faller & Kaylor (1966)	2	55	—	24	−15°
	1	118	—	11	10°–12°
Lilly (1966)	2	55	0.187	21	−20°
	1	110	0.050	11.9	7.5°
Iooss *et al.*(1978)	2	54.2	0.195	19.88	−23.3°
Present paper	2	54.15504	0.19489	19.869	−23.3261°
	1	112.75847	0.05182	11.397	7.2021°

TABLE 2. A summary of theoretical results for the Ekman instability

of the eigenstate is determined by minimization of R under the constraint that the determinant vanishes. Here an algorithm developed by Powell (1978) for nonlinear constrained optimization applies. It is most successful when it is applied to starting points that almost fulfil the constraint. The critical points obtained are listed in table 2 together with some existing theoretical results from the literature.

Near the critical points, $\partial R/\partial\epsilon$, $\partial R/\partial\alpha$ and $\partial R/\partial c_r$ are very small; therefore R can be found with a higher precision than the other parameters. Starting from different points, 12 digits of R and half as many on c_r, α and ϵ could be reproduced. The parameter values for which table 1 is calculated correspond to the critical type-2 point, and it is seen that the constraint is actually satisfied.

The maximum growth rate for a given value of R can be found by maximizing αc_i subject to the constraint that the determinant vanishes. Thus we have an optimization problem which depends on a parameter R. A continuation procedure combined with the above algorithm can be applied to follow the maximum growth rate as R increases above a critical value. The results are shown in figure 3.

On the surface of neutral stability, i.e. the surface in the (R, α, ϵ)-space along which c_i vanishes, contours of constant R are found by another continuation procedure. The arclength is introduced as a new parameter, and at fixed values of this parameter we search for a zero of the determinant along a line approximately orthogonal to the contour. For that purpose the modified Marquardt algorithm is used. Steps in the arclength are taken along the Euler chord and controlled by estimating the curvature. The least-square procedure is halted when the L_2 norm of the gradient of square sum becomes less than 10^{-10}. The value of the determinant is usually of order 10^{-12}–10^{-15} when the calculations end. Typically eight to ten evaluations of the determinant are needed per point on the contour. Figure 4 shows some representative contours of the neutral-stability surface.

The present results (figures 3 and 4) are in agreement with those of Lilly. However, they are more accurate and calculated in a qualitatively different way. Lilly's calculations are more complicated. He first finds $c = c_r + \alpha c_i$ as a function of the parameters R, α and ϵ. Then the neutral-stability surface can be computed from the equation

$$c_i(R, \alpha, \epsilon) = 0.$$

The use of standard numerical methods for eigenvalue problems dictates that procedure. In contrast, the present method involves only one transcendental equation

$$\det \boldsymbol{M}(R, \alpha, \epsilon, c_r) = 0.$$

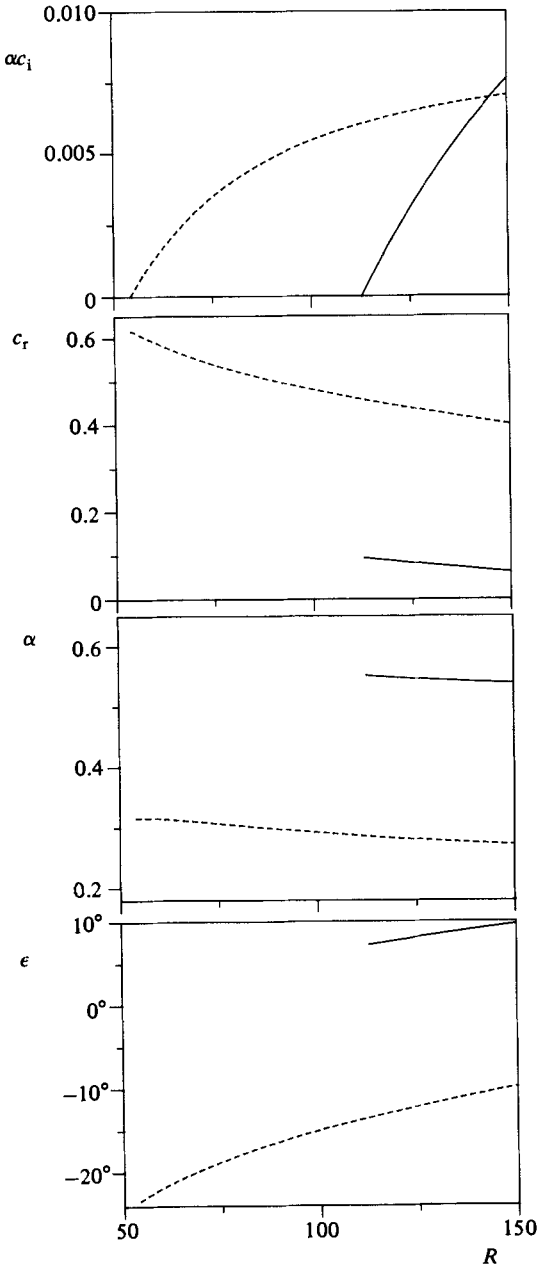

FIGURE 3. Maximum growth rate αc_i and the corresponding parameter values c_r, α and ϵ as functions of R are shown for both types of instabilities.

6. Discussion

The essential point of the approach described in this paper is that the linearly independent solutions of the problem (6) can be constructed as rapidly converging series (13) by a simple recurrence technique (12).

These analytical formulas, which involve little more than simple arithmetic operations on complex numbers, form a profitable basis for a numerical solution of

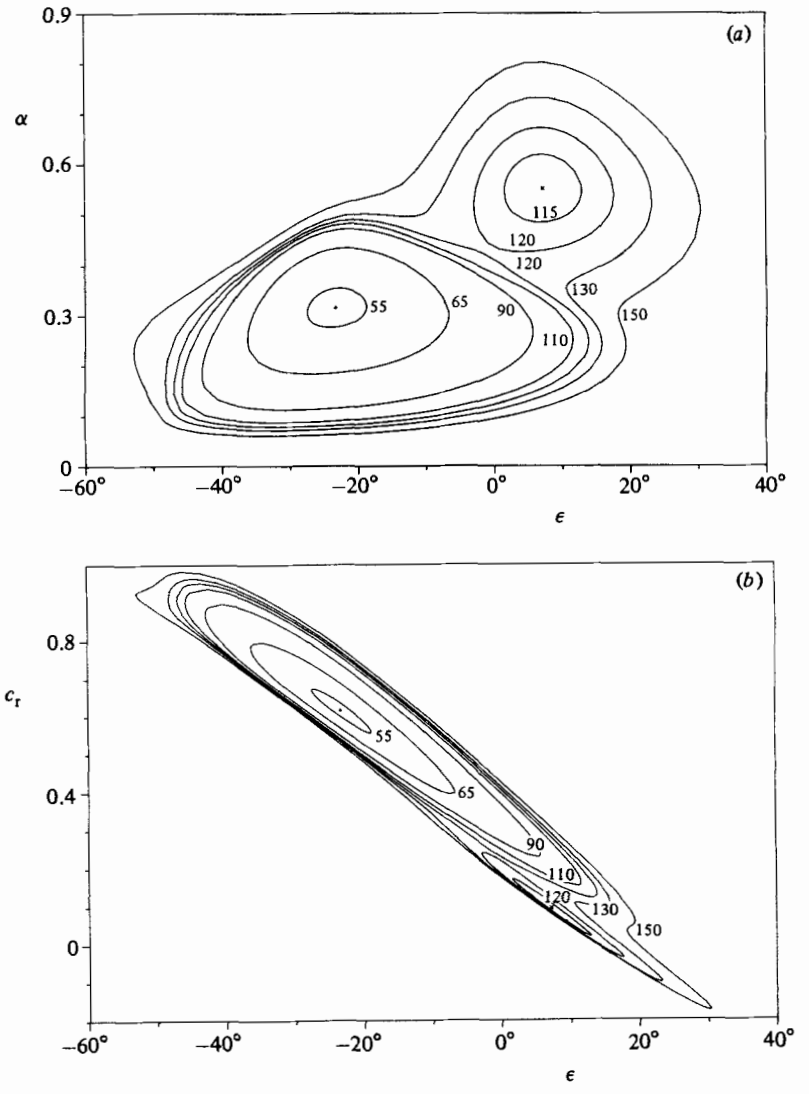

FIGURE 4. (*a*) The neutral-stability surface characterized by contours of constant R. The Ekman spiral is unstable to perturbations corresponding to parameter values inside the contours. If the parameter values for a perturbation lie outside the contours the perturbation will decay. The critical point is marked by (+) for the type-2 instability and by (×) for the type-1 instability. (*b*) The values of the phase velocity corresponding to the neutral stability curves shown in (*a*).

the stability problem, especially because the determination of the critical points, the neutral-stability surface, etc., naturally fall into the framework of numerical optimization algorithms, as shown in §5.

Before we discuss the applicability of the techniques to other problems, it is useful to recall the characteristic features of the present problem (6). First of all there is only one independent variable z and the problem is defined on a semi-infinite interval. The coefficients in the equation have a special form; they are constants or decaying complex exponential functions or a combination of both. Finally the problem is linear, homogeneous and it defines an implicit relationship between the parameters R, α, ϵ, c_r and c_i.

For a stability problem defined on a bounded interval, the basic solution will typically have a boundary layer near each end of the interval; therefore the coefficients will contain both growing and decaying exponential terms. This makes it impossible to find a recurrence formula based on decaying exponential functions. However, a recurrence formula in terms of orthogonal polynomials might in some cases be obtained easily, e.g. in the case of the Orr–Sommerfeld equation for the plane Poiseuille flow. Another approach to this problem is given by Roesner (1979).

The presented technique would probably involve too much computation if applied to a semi-infinite problem where the coefficients do not have the form described above.

All the parameters R, α, ϵ, c_r and c_i enter the computation principally on equal terms, so it is not significant whether (6) is an eigenvalue problem or not. A linear but inhomogeneous problem can be treated by the same technique because the fundamental matrix for the homogeneous problem can be found. Even some strongly nonlinear problems may be handled by a recurrence technique of the present type. An example is the equations describing the similarity solution to the problem of a rotationally symmetric flow above an infinite rotating disk.

The nonlinear stability analysis for the Ekman layer, as given by Iooss *et al.* (1970), is valid only in the neighbourhood of the critical point. It can be shown that a nonlinear extension of the present approach does not have such a restriction. Details of this approach are planned for a future paper.

I want to thank Dr H. B. Nielsen and Dr H. True for their suggestions and critical comments. I also like to thank the referees and Dr N. Arley for a useful criticism.

REFERENCES

FALLER, A. J. 1963 An experimental study of the instability of the laminar Ekman boundary layer. *J. Fluid Mech.* **15**, 560–576.

FALLER, A. J. & KAYLOR, R. E. 1966 A numerical study of the instability of the laminar Ekman boundary layer. *J. Atmos. Sci.* **23**, 466–480.

IOOSS, G., NIELSEN, H. B. & TRUE, 1978 Bifurcation of the stationary Ekman layer flow into a stable periodic flow. *Arch. Rat. Mech. Anal.* **68**, 227–256.

LILLY, D. K. 1966 On the instability of Ekman boundary flow. *J. Atmos. Sci.* **23**, 481–494 (1966).

POWELL, M. J. D. 1970 A hybrid method for non-linear equations. In *Numerical Methods for Non-linear Algebraic Equations* (ed. P. Rabinowitz), pp. 87–114. Gordon & Breach.

POWELL, M. J. D., 1978 A fast algorithm for non-linearly constrained optimization calculations. In *Proc. Biennial Conf. on Numerical Analysis, Dundee*, 1977 (ed. G. A. Watson). Lecture Notes in Mathematics, vol. 630, pp. 144–187. Springer.

ROESNER, K. G. 1979 An analytical approach to the determination of neutral stability curves. In *Recent Developments in Theoretical and Experimental Fluid Mechanics* (ed. U. Müller, K. G. Roesner & B. Schmidt), pp. 339–345. Springer.